ICSV13 - Vienna
The Thirteenth International Congress on Sound and Vibration
Vienna, Austria, July 2-6, 2006

SOUND TRANSMISSION LOSS MODEL OF CURVED MULTILAYERED PANELS

Frank Simon

ONERA Centre de Toulouse
2 avenue Edouard Belin, 31055 Toulouse, France
Frank.Simon@onecert.fr

Abstract

To improve the acoustic comfort into cabins of vehicle (aircraft or car), it can be interesting to class each sub-structure as a panel with simplified geometry (beam, flat panel, shell…). This allows to simulate more easily, with analytic models, the acoustic Transmission Loss (TL) of each structure and so to determine each contribution in the total internal noise. The TL represents the ratio between incident acoustic power applied on the structure and acoustic power radiated on the other side.Nevertheless, models generally consider the case of isotropic or multilayered flat panels (with process of homogenization) or cylinders with/without simple boundary conditions. These models are not suited to realistic structural and trim panels or multilayered windows with internal cavity, which are therefore simulated with Finite Element and Beam methods in low frequency range. Author has developed several analytic models to compute the TL of infinitely wide sandwich panels with multilayered laminates, in the case of diffused incident field in medium and high frequency ranges. Models consider elastic materials as, for example, homogeneous materials, composite fibres (kevlar, carbon or fibre glass) with resin, visco-elastic materials, honeycombs or foams, described by their stiffness matrix. They satisfy the continuity of displacements and shear stresses at the interface of each layer and use a cinematic approach and written of Lagrange equations. No process of homogenization is realized. This paper deals with a modification of the displacement field applied to previous models (with membrane, bending and shear terms) to take "curved" multilayered panels into account (generalisation of Love' theory).Tests of validation are led for different types of curved structure from theoretical and experimental bibliographic references. Moreover, the effect of shell radius is analysed through typical aircraft structures to determine real influence of geometry on acoustic TL.

INTRODUCTION

Most of models concern the behaviour of infinite or finite, cylinders described by circonferential modal models [1, 2]. These theories do not suited perfectly to curved

Eds.: J. Eberhardsteiner, H.A. Mang, H. Waubke

panels with lateral boundary conditions, contrary to [3] that proposes a model for an homogeneous finite curved stiffened panel. To take into account of aeronautic structures, several analytic models have been developed to compute the diffuse field Transmission Loss of orthotropic multi-layered flat panels [4]. Panels are assumed to be infinitely wide, which allows to have the behaviour in medium and high frequency bands, without defining particular boundary conditions, difficult to modelize in real condition.

The purpose of this paper is to introduce the effect of curvature for these types of structures into the previous model, thanks to Love theory [5, 6]: the developed model will be so dedicated as well to flat panels as curved panels.

THEORY

Each solid element of the curved panel is refered in (*s*,*z*,*r*) as precised in figure 1.

The direction of incident acoustic pressure (medium (1)) applied to the external surface is locally defined by angles θ and φ (wavenumber *k*). The induced structural wave is propagated across the panel surface in direction *x* (wavenumber $k_x = k\sin(\theta)$).

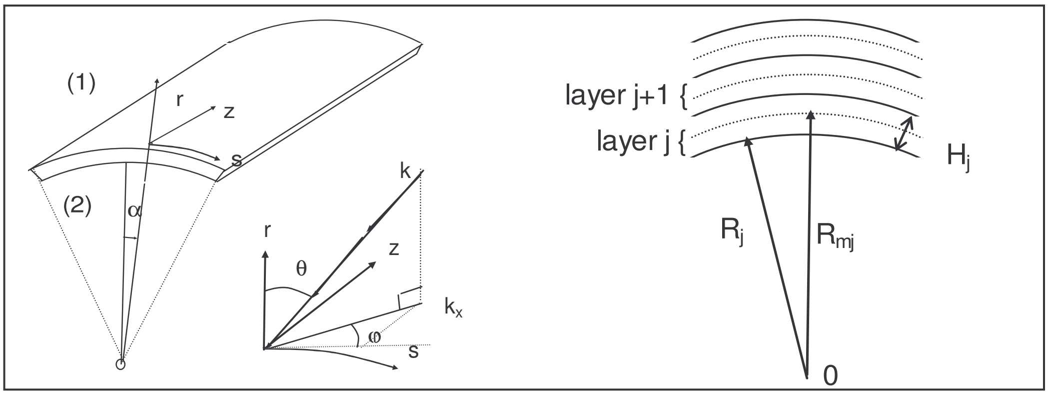

Figure 1 – Field and Structural system of coordinates (left) and Geometry of "Multi-layered" curved pane l (right)

The curved panel is composed of n orthotropic layers (figure 1). The displacement field can be written, as below, for each layer *j*:

$$\begin{cases} U_j(s,z,r) = U_j^s - \left(r - R_{m_j}\right)\left(-\dfrac{U_j^s}{R_j} + \dfrac{\partial W}{\partial s} + \Phi_j^s\right) \\ V_j(s,z,r) = U_j^z - \left(r - R_{m_j}\right)\left(\dfrac{\partial W}{\partial z} + \Phi_j^z\right) \\ W(s,z,r) = W(s,z) \end{cases} \quad (1)$$

with U_j, V_j, W displacements in *s*, *z* and *r* directions and R_{mj} median axis of a layer *j*.

The displacement in (*s*,*z*) includes membrane, bending and shear terms as for a multilayered flat panel [4]. The shell effect is introduced, along *s*, by the term $\frac{U_j^s}{R_j}$ with $R_j = R_{mj} - \frac{H_j}{2}$.

The normal and shear strains are the following:

$$\left\{\begin{array}{l} e_j^s = \frac{W}{R_j} + \frac{\partial U_j^s}{\partial s} + \left(r - R_{m_j}\right)\left(\frac{1}{R_j}\frac{\partial U_j^s}{\partial s} - \frac{\partial^2 W}{\partial s^2} - \frac{\partial \Phi_j^s}{\partial s}\right) \\ e_j^z = \frac{\partial U_j^z}{\partial z} - \left(r - R_{m_j}\right)\left(\frac{\partial^2 W}{\partial z^2} + \frac{\partial \Phi_j^z}{\partial z}\right) \\ \gamma_j^{zs} = \frac{\partial U_j^s}{\partial z} + \frac{\partial U_j^z}{\partial s} + \left(r - R_{m_j}\right)\left(\frac{1}{R_j}\frac{\partial U_j^s}{\partial z} - 2\frac{\partial^2 W}{\partial s \partial z} - \frac{\partial \Phi_j^s}{\partial z} - \frac{\partial \Phi_j^z}{\partial s}\right) \\ \gamma_j^{sr} = \frac{1}{R_j} U_j^s - \Phi_j^{sr} \\ \gamma_j^{zr} = -\Phi_j^{zr} \end{array}\right. \quad (2)$$

The stresses are related to the strains by the stiffness matrix as follows:

$$\begin{Bmatrix} \sigma_j^{ss} \\ \sigma_j^{zz} \\ \tau_j^{zr} \\ \tau_j^{sr} \\ \tau_j^{sz} \end{Bmatrix} = \begin{bmatrix} \bar{E}_j^{ss} & \bar{E}_j^{sz} & 0 & 0 & 0 \\ \bar{E}_j^{sz} & \bar{E}_j^{zz} & 0 & 0 & 0 \\ 0 & 0 & G_j^{zr} & 0 & 0 \\ 0 & 0 & 0 & G_j^{sr} & 0 \\ 0 & 0 & 0 & 0 & G_j^{sz} \end{bmatrix} \begin{Bmatrix} e_j^s \\ e_j^z \\ \gamma_j^{zr} \\ \gamma_j^{sr} \\ \gamma_j^{sz} \end{Bmatrix} \quad (3)$$

The matrix parameters are complex to take the damping loss factor η into account:

$$Mod_{complex} = Mod_{real}(1 - i\eta) \quad (4)$$

The hypothesis of plane strains in 2D (*s,z*) allows to determine the stiffnesses terms according to the elastic moduli , E_j^{ss} and E_j^{zz} , and the Poisson coefficient υ_j^{sz} :

$$\bar{E}_j^{ss} = \frac{E_j^{ss}}{1 - \frac{E_j^{ss}}{E_j^{zz}} \upsilon_j^{sz^2}} \ (5), \quad \bar{E}_j^{zz} = \frac{E_j^{zz}}{1 - \frac{E_j^{ss}}{E_j^{zz}} \upsilon_j^{sz^2}} \ (6), \quad \bar{E}_j^{sz} = \upsilon_j^{sz} \bar{E}_j^{ss} \ (7)$$

We assume the continuity of displacements between layers *j* and *j+1* by an iterative procedure:

$$\left\{\begin{array}{l} U_j^s - \frac{H_j}{2}\left(-\frac{U_j^s}{R_j} + \frac{\partial W}{\partial s} + \Phi_j^s\right) = U_{j+1}^s + \frac{H_{j+1}}{2}\left(-\frac{U_{j+1}^s}{R_j} + \frac{\partial W}{\partial s} + \Phi_{j+1}^s\right) \\ U_j^z - \frac{H_j}{2}\left(\frac{\partial W}{\partial z} + \Phi_j^z\right) = U_{j+1}^z + \frac{H_{j+1}}{2}\left(\frac{\partial W}{\partial z} + \Phi_{j+1}^z\right) \end{array}\right. \quad (8)$$

Moreover, the continuity of shear stress between layers is assured in direction of propagation *x*, in neglicting the effect of curvature, as:

$$G_j^{xr} \Phi_j^{xr} = G_{j+1}^{xr} \Phi_{j+1}^{xr} \text{ with } G_{j,j+1}^{xr} = \cos^2(\varphi) G_{j,j+1}^{sr} + \sin^2(\varphi) G_{j,j+1}^{zr} \quad (9)$$

So, parameters of a layer *j* can be written in function of parameters of the layer *1* (U_0, W_0 and Φ_0):

$$\begin{cases} U_j^s = A_j U_1^s - B_j \dfrac{\partial W}{\partial s} - C_j \Phi_1^s \\ U_j^z = U_1^z - C_j \dfrac{\partial W}{\partial z} - D_j \Phi_1^z \end{cases} \quad (10) \quad \text{with} \quad \begin{cases} \begin{Bmatrix} U_1^s \\ U_1^z \end{Bmatrix} = U_0 \begin{Bmatrix} \cos(\varphi) \\ \sin(\varphi) \end{Bmatrix} \cos(k_x(\cos(\varphi)s + \sin(\varphi)z)) \\ W = W^0 \sin(k_x(\cos(\varphi)s + \sin(\varphi)z)) \\ \begin{Bmatrix} \Phi_1^s \\ \Phi_1^z \end{Bmatrix} = \Phi_0 \begin{Bmatrix} \cos(\varphi) \\ \sin(\varphi) \end{Bmatrix} \cos(k_x(\cos(\varphi)s + \sin(\varphi)z)) \end{cases} \quad (11)$$

The potential and kinetic energy densities, Ep_j and Ec_j, can be expressed by:

$$\begin{aligned} Ep_j &= \frac{1}{2}\left(\overline{E}_j^{ss} {e_j^s}^2 + \overline{E}_j^{zz} {e_j^z}^2 + 2\overline{E}_j^{sz} e_j^s e_j^z + G^{sz} {\gamma_j^{sz}}^2 + G_j^{zr} {\gamma_j^{zr}}^2 + G_j^{sr} {\gamma_j^{sr}}^2\right) \\ Ec_j &= \frac{1}{2}\rho\left({\dot{U}_j^s}^2 + {\dot{U}_j^z}^2 + \dot{W}^2\right) \end{aligned} \quad (12)$$

The potential energy (PE) and the kinetic energy (KE) are calculated by integrating the different energy densities over a volume defined by the thickness of the panel (*r* direction), one wavelength in s and z directions.

The Lagrange‘s equations are then used to obtain the parameters U_0, W_0 and Φ_0:

$$\left(\frac{d}{dt}\right)\left(\frac{\partial KE}{\partial \dot{g}r}\right) - \frac{\partial KE}{\partial gr} + \frac{\partial PE}{\partial gr} = Qr \quad (13)$$

with g_r corresponding to U_0, W_0 and Φ_0 (generalized displacements) and Qr the generalized forces coming from the pressures $p_1(s,z)$ et $p_2(s,z)$ acting respectively on the faces in contact with media (1) and (2):

$$Q_r = \begin{Bmatrix} 0 \\ \displaystyle\int_0^{\lambda_z}\int_0^{\lambda_s} (p_2(s,z) - p_1(s,z))\, W(s,z)\, ds\, dz \\ 0 \end{Bmatrix} \text{ with } p_{1,2}(s,z) = P_{1,2} \sin(k_x(\cos(\varphi)s + \sin(\varphi)z)) \quad (14)$$

With the Sommerfeld conditions, the acoustic transmission coefficient can be described by $\tau(\theta,\varphi) = \dfrac{W_T}{W_I}$ (15) (with W_I and W_T the incident and transmitted acoustic powers).

Like in [4],

$$\tau(\theta,\varphi) = \left(\frac{\omega\rho_{air} c_{air}}{\cos\theta}\right)^2 \frac{4}{\left|Z_s - 2i\,\dfrac{\omega\rho_{air} c_{air}}{\cos\theta}\right|^2} \quad (16)$$

with ω circular frequency and $Z_s = \dfrac{p_2 - p_1}{W_0}$

In our case, we are interested in a diffuse field excitation. So, the transmission coefficient must be averaged over incidence orientation as follows, to obtain the diffuse field Transmission Loss:

$$TL = -10\log\left(\frac{\int_0^{2\pi}\int_0^{\theta\lim} \tau(\theta,\varphi)\sin(\theta)\cos(\theta)\, d\theta\, d\varphi}{\int_0^{2\pi}\int_0^{\theta\lim} \sin(\theta)\cos(\theta)\, d\theta\, d\varphi}\right) dB \text{ with } \theta_{\lim} \le 90° \quad (17)$$

SIMULATIONS

Validation with literature results

The TL can reach low values around two particular frequencies:
At the first one, called the ring frequency f_a, the transverse displacement W induced a strain in s direction and a propagation of longitudinal waves, for which, the wavelength corresponds to cylinder perimeter.
At the second one (generally higher), called the critical frequency f_c, the celerity of bending waves is equal to celerity of acoustic waves.
So: $f_a = \frac{1}{2\pi R} \cdot \sqrt{E / \rho\left(1-\nu^2\right)}$ (18) and $f_c = \frac{c_{air}^2}{2\pi}\sqrt{\frac{\rho H}{D}}$ (19) with D bending rigidity for homogeneous structures.
The effect of curvature occurs generally in low frequency bands. It is assumed that, when the frequency is higher than about two times of the ring frequency, the TL is similar to a flat panel [3].

[7] compares the TL obtained experimentally at Third Octave frequencies for a curved glass panel with a radius of 1.8 m and for a flat glass panel (surface : 0.86 x 0.86 m²). The sample thickness is 4 mm for both.
Simulations are led for the flat panel thanks to a large value of radius.
Present model (figure 2) gives quite close results, except around the 1st structural resonance frequency (f_{11}), which is not taken into account. The influence of curvature is noticeable up to about two times of the ring frequency ($f_a \sim 480$ Hz), as expected. Moreover, the curved and flat panels have similar critical frequencies ($f_c \sim 3200$ Hz).

Simulation results are then compared with [8] experimental results. Experiments have been led for two curved aluminium panels (thickness: 1mm) with respectively a radius of 1 m and 4 m (surfaces: 0.87 x 0.95 m² / 0.87 x 0.91 m²). For the highest radius, theory with curvature effect (figure 3) is not justified: the TL is highly underestimated around the ring frequency ($f_a \sim 200$ Hz), contrary to TL relative to a flat panel, because of closeness of the 1st resonance frequencies. But, for the lowest radius, the ring frequency appears logically at four times of the previous ring frequency ($f_a \sim 800$ Hz) and the theory is representative of experimental results. As for glass panels, the theoretical behaviours of curved and flat panels are similar from two times of the ring frequency.

The model is finally applied to an orthotropic cylinder (single layer) simulated in [1] (figure 4) and to isotropic, orthotropic (single layer) and composite sandwich cylinders simulated in [2] (figure 5). While present model does not consider circonferential shell modes, contrary to [1] and [2], simulations are representatives of general behaviour. One can notice a constant difference (~ 3 dB) with [10] results, certainly due to different TL formulations.

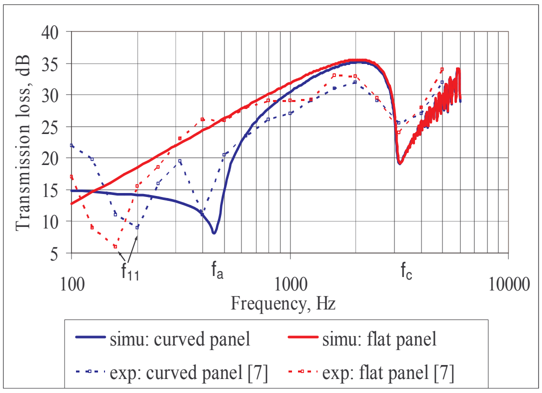

Figure 2 – Simulated TL compared with [7]

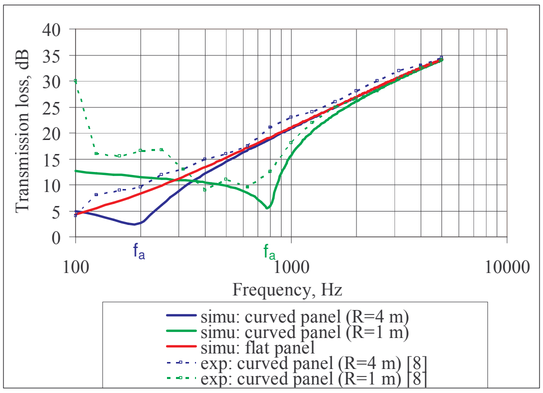

Figure 3 – Simulated TL compared with [8]

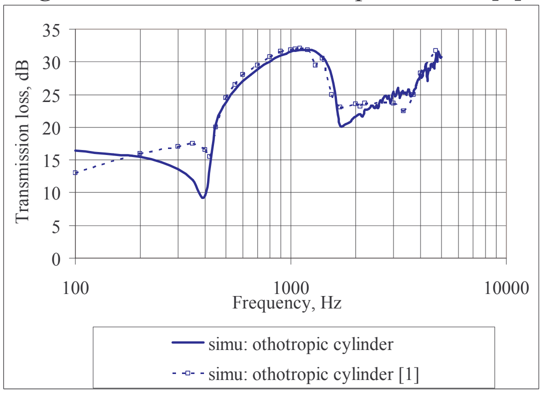

Figure 4 – Simulated TL compared with [1]

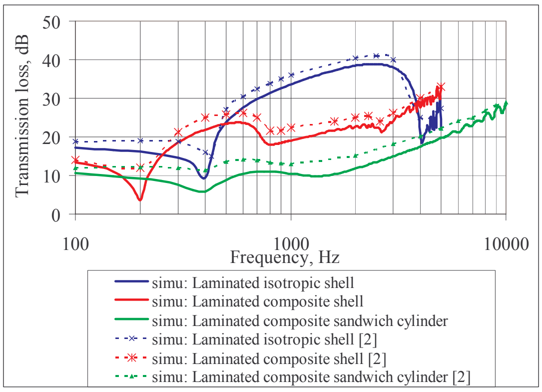

Figure 5 – Simulated TL compared with [2]

Remarks: literature results are extracted directly from figures of used references.

Behaviour of airplane structures

The simulations are now applied to a typical airplane sidewall fuselage, whose the characteristics are as following (figure 6):

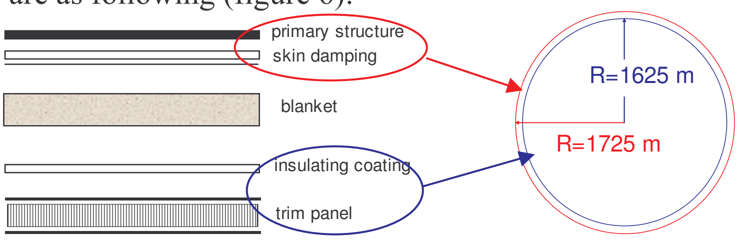

Figure 6 - Typical airplane sidewall fuselage

The stringers and frames are neglected and we assume that the “diffused field" TL is realistic of an "incoherent" external excitation (mainly turbulent boundary layer).
First, we simulate the behaviour of a primary structure provided with a skin damping (A), then, the behaviour of trim panels with or without insulating coating (respectively (B) and (C)) (figure 7). Configurations of trim panels result from an optimisation led with industrial requirements (surfacic mass and thickness up to about 4 kg/m^2 and 20 mm, aeronautic materials). The mechanical and dimensional

characteristics of different layers are specified in table 1. One can notice, for the different structures, that the effect of curvature is present up to1000 Hz and that the ring frequencies, obtained between 200 and 450 Hz, are close to frequencies computed by (18) with mean young modulus and density. Moreover, the behaviour due to the bending stiffness of primary structure with skin damping (A) appears only from about 4000 Hz: below this frequency, the high loss factor of EAR foam layer has not influence on the "diffuse sound field" TL (figure 8). The EAR visco-elastic layer, used generally to absorb vibrations, is not suited to increase TL of panel (B), the panel critical frequency being higher than 10 kHz (figure 8). One can see, also, that the chosen direction of honeycomb cells with respect to (*s,z*) is not important, in spite of natural orthotropy. Finally, the values of honeycomb shear moduli of (C) are preponderant from 1000 Hz (figure 9): With Nomex honeycomb 1, appears a wide critical frequency band (celerity of bending waves close to celerity of acoustic waves), contrary to Nomex honeycomb 2. So, higher are the shear moduli, lower is the TL. The fact that "curvature" and "honeycomb shear moduli" effects are dissociated in frequency validates the hypothesis introduced in (9).

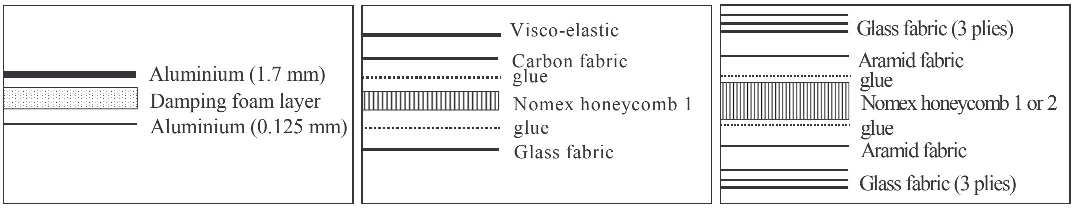

Figure 7 - Configurations of (A) (left), (B) (middle) and (C) (right)

Table 1 – Mechanical and dimensional characteristics of sidewall layers used for simulations

Layer \ Parameter	Glass fabric	Aramid fabric	Carbon fabric	Nomex honey-comb 1	Nomex honey-comb 2	glue	EAR Visco-elastic	EAR Damping foam
$\rho\,(kg/m^3)$	1600	1300	1500	48	32	1000	1714	104
$t\,(mm)$	0.22	0.186	0.27	5 mm (B) 10 mm (C)	10 mm	0.25	1.27	6.35
$E_{ss}\,(Mpa)$	16200	27500	46000	~1	~1	1680	880	6.8
$E_{zz}\,(Mpa)$	16200	27500	46000	~1	~1	1680	880	6.8
υ	0.15	0.09	0.08	~ 0	~ 0	0.4	~ 0	~ 0
$G_{zr}\,(Mpa)$	2750	2000	3100	24	13	600	260	1.8
$G_{sr}\,(Mpa)$	2750	2000	3100	45	23	600	260	1.8
$G_{sz}\,(Mpa)$	2750	2000	3100	~1	~1	600	260	1.8
$\eta\,(\%)$	1	1	1	3	3	1	47	50

CONCLUSION

A model of acoustic Transmission Loss taking into account of curvature effect for multi-layered panels has been presented. It is a generalization of a previous model suited, for example, to flat sandwich panels (validated by specific experimentations

[4]), with a low computational cost (compared to [10]). While neglecting the boundary conditions, theoretical predictions agree well with experimental results applied to particular homogeneous curved panels, thus above the first resonance frequencies. The application to typical airplane structures has shown that the "curvature" effect and the influence of the shear strain and stress introduced by honeycombs in trim panels appear in separated frequency bands (respectively before and after 1000 Hz, for given structures with honeycomb). The curvature effect seems noticeably prejudicial for airplane internal noise. Nevertheless, these tendencies must rely on experimental results to be confirmed and the theoretical approach be used in a global model taken into account primary structure and trim panel coupled with blanket (figure 4).

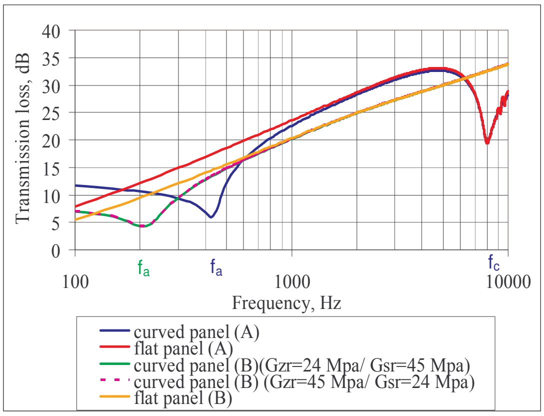

Figure 8 - Simulated TL for (A) and (B)

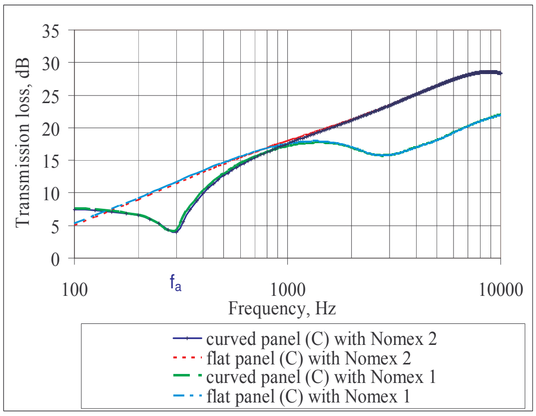

Figure 9 - Simulated TL for (C)

REFERENCES

[1] A. Blaise, C. Lesueur, M. Gotteland, M. Barbe, "On sound transmission into an orthotropic infinite shell: comparison with Koval's results and understanding of phenomena", J. Sound Vib., **150(2)**, 233-243 (1991).

[2] S. Ghinet, N. Atalla, H. Osman, "Diffuse field transmission into infinite sandwich composite and laminate composite cylinders", J. Sound Vib., **289**, 745-778 (2006).

[3] B. Liu, L. Feng, A. Nilsson, "Influence of pressurization on sound insulation of curved airplane panels", Proceeding of ICSV12, Lisbon (2005).

[4] F. Simon, S. Pauzin, D. Biron, "Optimisation of sandwich trim panels for reducing helicopter internal noise", Proceeding of ERF30, Marseille, (2004).

[5] A.E.H Love, *A Treatise on the Mathematical Theory of Elasticity (*Dover Publ., New-York, 1940).

[6] S. J. Walsh, R. G. White, " Beam with constant curvature", J. Sound Vib., **221**, 887-899 (1999).

[7] J. C. Pascal, "Le choix des vitrages pour l'isolation acoustique des habitacles d'engins", Recueil de conférences de "Matériaux pour l'isolation acoustique des machines et des véhicules", Publication CETIM" (1995).

[8] B. Liu, L. Feng, A. Nilsson, "Sound transmission through aircraft panels with stringer and ring frame attachments" accepted for publication in J. Sound Vib (2006).